R0840008 2

CENTRAL INSTITUTE OF PHYSICS

INSTITUTE FOR PHYSICS AND NUCLEAR ENGINEERING*)

Bucharest, POB MG-6, ROMANIA

and

BUCHAREST UNIVERSITY**)

DEPARTMENT OF NUCLEAR PHYSICS

Bucharest, POB MG-6, ROMANIA

IFIN - FT-204-1981 September

Experimental evidence for dual diffractive resonances in nucleon-nucleus scattering

D.B.ION) and R.ION-MIHAI*)*

Abstract : Experimental data on nucleon-nucleus scattering for laboratory momenta between 0.9:10 GeV/c are analysed in terms of the dual diffractive resonance (DDR) mechanism. The experimental data for all the nuclei are found to agree well with the predictions of the collective DDR states dominance.

1. INTRODUCTION

In two recent papers /1,2/ we introduced new exotic collective states of the nucleus called dual diffractive resonances (DDR) which can be excited in the hadron-nucleus interactions. The experimental data /3,13/ on pion-nucleus scattering in the region corresponding to the Δ(1236) resonance in the elementary interaction, are analysed in ref. /14/ from the point of view of the excitation of the collective DDR states of the nucleus. Then, the experimental data for all the nuclei are found consistent with the hypothesis of the DDR dominance in the pion-nucleus scattering in the Δ(1236) resonance region. The DDR description of the hadron-nucleus scattering, at energies corresponding to the elementary hadron-nucleon resonances, provides a new calculationally powerful techniques by which we can understand the new kind of duality manifested by the resonant energy behaviour of the total elastic and total inelastic cross sections as well as of all the hadron-nucleus partial waves /13,15-17/, and by the diffraction patterns of the differential cross sections /3-5, 13/. The DDR state approach is not only an interesting picture capable of quantitative results but also affords physical insight into the many body dynamics and, in the first approximation incorporates simultaneously two essential controlling aspects of the scattering: the resonance and diffraction patterns.

In this paper the experimental data on the nucleon-nucleus scattering, for laboratory momenta between 0.9 and 10 GeV/c are analysed in terms of the DDR predictions/1,2, 14/. The essential characteristic features of the collective DDR states domainance are presented in sect.2 while the agreement between DDR mechanism and the experimental data is discussed in sect.3.

2. THE DDR PREDICTIONS

The dual diffractive resonance (DDR) phenomena, which can occur especially in the hadron-nucleus scattering as an effect of the "spreading" of the elementary hadron-nucleon resonances over all hadron-nucleus partial waves, are described by the following remarkable amplitude /1/

$$F(E,\cos\theta)=\frac{\lambda}{2}(l_0+1)^2\,\frac{\Gamma_{el}\,\langle P_l(x)\rangle}{E_0-E-\frac{i}{2}\left[\Gamma-\gamma_0(E_0-E)\right]}\,, \qquad (1)$$

where

$$\langle P_l(x)\rangle=\frac{\sum_{l=0}^{l_0}(2l+1)\,P_l(\cos\theta)}{\sum_{l=0}^{l_0}(2l+1)}=\frac{\dot P_{l_0+1}(x)+\dot P_{l_0}(x)}{(l_0+1)^2}\,, \qquad (2)$$

$$E+m_A-m_N=\left[m_k^2+k^2\right]^{1/2}+\left[m_A^2+k^2\right]^{1/2}\equiv W\,, \qquad (3)$$

$x=\cos\theta$, $\dot P_l(x)=dP_l(x)/dx$, $P_l(x)$ are Legendre polynomials, w and k are the c.m.energy and momentum, $\lambda=1/k$, θ is the c.m. scattering angle, m_A, m_N, m_h are the masses of the nucleus, nucleon and incident hadron respectively, $l_0(=kR)$ is the maximum value of the angular momentum while $E_0+m_A-m_N$, Γ, Γ_{el} and γ_0 are the effective parameters (mass, total width, elastic width and asymmetry) of the "induced resonances" in each hadron-nucleus partial wave. The asymmetry parameter γ_0 is a dimensionless parameter /1/ defined in a natural way starting with a Regge representation for each hadron-nucleus partial wave from which we have $\gamma_l^{\ell}=2\,J_m\dot\alpha(E_0)/R_0\dot\alpha(E_0)$, $\dot\alpha_l(E)=d\alpha_l(E)/dE$.

Now using eqs (1,2), we obtain the following important DDR predictions /1,2/:

(I) The total σ_T, elastic σ_{el}, inelastic σ_{in} cross sections as well as the ratio of the real and the imaginary parts of the forward hadron-nucleus scattering have a resonant behaviour described by

$$\sigma_T = \pi \lambda^2 (l_0+1)^2 \quad \frac{\Gamma_{el}\,[\Gamma - \gamma_0 (E_0 - E)]}{(E_0-E)^2 + \frac{1}{4}[\Gamma - \gamma_0 (E_0-E)]^2} \tag{4}$$

$$\sigma_{el} = \pi \lambda^2 (l_0+1)^2 \quad \frac{\Gamma_{el}^2}{(E_0-E)^2 + [\Gamma - \gamma_0 (E_0-E)]^2}, \tag{5}$$

$\sigma_{in} = \sigma_T - \sigma_{el}$, and

$$\alpha = \frac{Re\, F(0^\circ)}{Im\, F(0^\circ)} = \frac{2(E_0 - E)}{\Gamma - \gamma_0 (E_0 - E)}, \tag{6}$$

respectively.

(II) The angular distributions of the collective DDR states have typical diffractive patterns described by

$$\frac{d\sigma_{el}(\theta)}{d\Omega} = \frac{\sigma_{el}\,(l_0+1)^2}{4\pi} \left| < P_{l_0}(\cos\theta) > \right|^2 \tag{7a}$$

They are very sensitive to the values of the angular momentum $l_0 \simeq kR$. The number of the maxima and minima in the entire cos θ region are given by $N_{max} = l_0 + 1$, $N_{min} = l_0$, (see fig.1, ref /1/). The angular distributions of the DDR states as well as those of the dual diffractive scattering (DDS) phenomena /2/ have pronunced forward-backward asymmetry chardcterized by

$$\frac{d\sigma_{el}}{d\Omega}(0^\circ) = (l_0+1)^2 \frac{d\sigma_{el}}{d\Omega}(180^\circ) = \frac{\sigma_{el}\,(l_0+1)^2}{4\pi}. \tag{7b}$$

The logarithmic slope of the forward diffraction peak for the DDR and DDS phenomena is described by the relation:

$$b_{DDR} = b_{DDS} = \frac{\lambda^2}{4}\left[\frac{4\pi}{\sigma_{el}} \cdot \frac{d\sigma_{el}}{d\Omega}(0°) - 1\right] . \qquad (7c)$$

Note that eq.(7c) is obtained from eqs. (7a,b) by using the definition of the logarithmic slope of the forward peak, indeed, we have

$$b_{DDR} = b_{DDS} = \frac{d}{dt}\left[\ell n \frac{d\sigma_{el}}{d\Omega}(\theta)\right]\Big|_{t=0} = 2\frac{d}{dt}\left[< P_\ell (\cos(\theta)>\right]\Big|_{t=0}$$

$$= \lambda^2 \frac{\ddot{P}_{\ell_0+1}(1) + \ddot{P}_{\ell_0}(1)}{(\ell_0+1)^2} = \frac{\lambda^2}{4}\ell_0(\ell_0+2)$$

from which we get the result (7c) since

$$\ddot{P}_{\ell_0+1}(1) + \ddot{P}_{\ell_0}(1) = \frac{\ell_0(\ell_0+1)^2(\ell_0+2)}{4} ,$$

and

$$\ell_0(\ell_0+2) = (\ell_0+1)^2 - 1 = \frac{4\pi}{\sigma_{el}} \cdot \frac{d\sigma_{el}}{d\Omega}(0°) - 1 .$$

(iii) The collective DDR states saturate the "axiomatic" bounds

$$\sigma_T^2 \leq 4\pi\lambda^2(\ell_0+1)^2(1+\alpha^2)^{-1}\sigma_{el} \qquad (8a)$$

$$\Gamma_{(hA)} \leq \Gamma_{(hN)} A^{1/3} , \quad \Gamma(hA) \equiv \Gamma , \qquad (8b)$$

where $\Gamma(hN)$ is the total width of the elementary hadron-nucleon resonance and A is the number of the nucleons in nucleus.

For $E = E_o$ the logarithmic slope (7c) and the bound (8a) become

$$b_{DDR}(E_o) = \frac{1}{4}\left[\frac{\sigma_{To}}{4\pi\sigma_{elo}} - \lambda^2\right], \tag{9a}$$

and

$$\sigma_{To} \leq 4\pi\lambda^2(l_o+1)^2\sigma_{elo}, \tag{9b}$$

where σ_{To} and σ_{elo} are the total and elastic cross sections at $E = E_o$.

Next, for $\Gamma = 2\Gamma_{el}$, $E = E_o$ and $l_o = kR \gg 1$, from eqs.(4)-(9) we get the strong absorption limit:

$$\sigma_T = 2\sigma_{el} = 2\sigma_{in} = 2\pi(R+\lambda)^2, \quad \alpha = 0, \quad b_{DDR} \simeq \frac{R^2}{4}, \tag{10a}$$

$$\frac{d\sigma_{el}}{d\Omega}(\theta) = \frac{d\sigma_{el}}{d\Omega}(0^\circ)\left[\frac{2J_1[(R+\lambda)q]}{(R+\lambda)q}\right]^2, \quad q \equiv \sqrt{-t} = 2k\sin\theta. \tag{10b}$$

where $J_1[(R+\lambda)q]$ is the Besselfunction of order 1.

Therefore, in this case, the strong absorption limit is obtained just as a coherent superposition of l_o overlapping resonances degenerate in position.

3. COMPARISON WITH EXPERIMENT

Now, let us examine the energy behaviour of the experimental data of the nucleon-nucleus scattering in the region of the laboratory momenta $p_{LAB} = 0.9 \div 10$ GeV/c. The experimental data on the nucleon-nucleus total cross sections /18-40/ are presented in figs. 1-12. The total cross sections for all nuclei exhibit a maximum

clearly related with the maximum observed in the nucleon-nucleon total cross sections (e.g. neutron-proton total cross sections, see fig.1). In fitting eq.(4) to the experimental data we have taken: E_o=2350 MeV, $\Gamma_{el} = \gamma_1 k$, $\Gamma = \Gamma_{np} A^{1/3}$, with Γ_{np}=5678.4 MeV since a three parameter ($\gamma_o, \gamma_1, \Gamma$) fit to the experimental data/41/ on np total cross sections in the range of p_{LAB}=0.9GeV/c to 10 GeV/c gives the result: Γ=(5678.4 ± 212.3) MeV. The geometric size R, from the definition $l_o = kR$, was fixed as in tables 1 and 2, equal to the equivalent spherical radius /42/ of each nucleus. The other parameters γ_o and γ_1 from eq. (4) are allowed to vary for each nucleus in order to obtain the best X^2 - fit of the total cross sections. The best parameters γ_o and γ_1 are given in tables 1a, 1b and 2, Next, using these parameters in eqs. (5), $\sigma_{in}=\sigma_T-\sigma_{el}$, (6) and (7c), we obtain the absolute predictions of σ_{el}, σ_{in}, α and b_{DDR}, respectively. These results for σ_{el}, σ_{in} and α are also indicated by curves in figs. 1-12. From all these results (see figs. 1-12 and tables 1,2) we see that all the DDR predictions (excepting those for nD) are in excelent agreement with the available experimental data on the total σ_T/18 - 41/, elastic /20, 26, 28, 29, 44,46-50/ and inelastic /20, 21, 26, 28, 29, 44, 46-50/ cross sections. The experimental data on the ratio α for the neutron-proton/51 - 55/ and proton-nucleus scattering /55 - 60/ are very well reproduced by the DDR mechanism but more experimental data are required.

Next, the experimental nucleon-nucleus angular distributions in the laboratory momenta p_{LAB} = 0.9 ÷ 10 GeV/c displays typical diffraction patterns: a periodic side maxima and minima with a pronunced forward peak. All these characteristic features are well described by the DDR predictions: eq. (7a). A quantitative analysis of the experimental data /43/ on the logarithmic slope of the forward

diffraction peek in terms of the DDR predictions (7c) is presented in fig. 13. Then, we see that the b_{DDR} slopes are in good agreement with the results of ref. /43/. A fit of the parameters γ_o and γ_1 shows that they behave systematicaly (see fig. 14) as: $\gamma_o = 2.322\ A^{0.483}$ and $\gamma_1 = 0.650\ A^{0.572}$, where A is the number of the nucleons in nucleus. From all the above results we see that the available experimental data for all the nuclei are consistent with the hypothesis of the DDR dominance in the nucleon-nucleus scattering in the region $p_{LAB} = 0.9 \div 10$ GeV/c.

3. CONCLUSIONS

In the preceding sections of this paper we analysed the nucleon-nucleus scattering from the point of view of the dominance of the collective DDR states of the nucleus. Then, we have obtained the following important results.

(I) The nucleon-nucleus total cross sections (see figs. 1-12, and tables 1,2) for $p_{LAB} = 0.9 \div 10$ GeV/c are consistent with the DDR predictions: eq.(4) with $\Gamma = \Gamma_{np} A^{1/3}$, $\Gamma_{np} = 5678.4$ MeV, $E_o = 2350$ MeV and the geometric size R fixed as in talbes 1-2. The parameters γ_o and γ_1 are described by $\gamma_o = 2.322\ A^{0.483}$ and $\gamma_1 = 0.650\ A^{0.572}$ (see fig. 14).

(II) The experimental data on the nucleon-nucleus elastic σ_{el}, inelastic σ_{in}, cross sections and also on the ratio σ_{el}/σ_{in} for $p_{LAB} = 0.9 \div 10$ GeV/c, are found in good agreement with the DDR mechanism: eqs. (5), $\sigma_{in} = \sigma_T - \sigma_{el}$ and (6) with the parameters obtained by the fit of the total cross sections.

(III) The experimental data /43/ on the logarithmic slope of the neutron-nucleus forward differential peak, for $p_{LAB} \simeq 0.9 \div 10$ GeV/c, are well reproduced (see fig. 13 and tables 1-2) by the predictions of the collective DDR states dominance: eq. (7c), but more experimental data are required.

We note of course that, for a quantitative analysis of the polarized and unpolarized angular distributions on the basis of the DDR mechanism it is first necessary to extend the above DDR predictions to include the spin effects and the electromagnetic corrections.

REFERENCES

/1/ D.B.Ion, Rev.Roum.Phys. 26 (1981) 15.

/2/ D.B.Ion, Rev.Roum.Phys. 26 (1981) 25

/3/ F.Binon et al., Nucl.Phys. B17 (1970) 168; B33 (1971) 42; B40 (1972) 608.

/4/ R.W.Bercaw et al., Phys.Rev.Lett. 29 (1972) 1031

/5/ M.L.Scott et al., Phys.Rev.Lett. 28 (1972) 1209.

/6/ C.Wilkin et al., Nucl.Phys. B62 (1973) 61.

/7/ B.W.Allardice et al., Nucl.Phys., A209 (1973) 1.

/8/ A.S.Clough et al., Nucl. Phys. B76 (1974) 15.

/9/ F.Balestra et al., Nuovo Cim. A12 (1975) 351; A13 (1975) 673.

/10/ Yu.A.Sherbakov et al., Nuovo Cim. A31 (1976) 242; A31 (1976) 249.

/11/ A.S.Carroll et al., Phys.Rev.14C (1976) 635.

/12/ I.V.Folomkin et al., Nuovo Cim. A43 (1978) 499.

/13/ F.Binon et al., Nucl.Phys. A298 (1978) 499

/14/ D.S.Ion and R.Ion-Mihai, Nucl.Phys. A360 (1981) 400.

/15/ I.V.Folomkin et a ., Nuovo Cim. Lett. 5 (1972) 1125.

/16/ R.H.Landau et al., Ann.Phys. (N.Y.) 78 (1973) 299.

/17/ M.H.Höenig et al., Phys.Rev. 10C (1974) 2102..

/18/ V.A.Nedzel, Phys.Rev. 94 (1954) 174; Phys.Rev.91 (1953) 440.

/19/ V.P.Dzhelopov et al., Dokl.Akad.Nauk SSSR 104 (1955)717.

/20/ T.Coor et al.,Phys.Rev.98 (1955) 1369.

/21/ W.Schimmerling et al., Phys.Rev. C7 (1973) 248.

/22/ W.Schimmerling et al., Phys.Lett. 37B (1971) 177.

/23/ E.F.Parker et al., Phys.Lett. 31B (1970)246,250.

/24/ J.Engler et al., Phys.Lett. 32B (1970) 716.

/25/ J.Engler et al., Phys.Lett. 28B (1968) 64.

/26/ N.E.Booth et al., Proc.Phys.Soc. A71 (1958) 293

/27/ W.L.Lakin et al., Phys.Letters 31B (1970) 677.

/28/ W.S.Pantuev et al., J.E.T.P. 42 (1962) 909.

/29/ J.H.Atkinson et al., Phys.Rev.123 (1961) 1850.

/30/ T.Schwaller et al., Nucl.Phys. A316 (1979) 317.

/31/ M.S.Kozodaev et al., JETP 38 (1960) 708.

/32/ L.Riddiford et al., Proc.Roy.Soc.A257 (1960) 316.

/33/ G.J.Igo et al., Phys.Rev.Lett. 18 (1967) 1200.

/34/ M.J.Longo et al., Phys.Rev. 125 (1962) 701.

/35/ C.J.Batty et al., Proc.Phys.Soc., 73 (1958) 100.

/36/ M.E.Low et al., Nucl.Phys.9 (1958/60) 600.

/37/ N.E.Booth et al., Proc.Phys.Soc. A70 (1957) 209.

/38/ J.Marschall et al., Phys.Rev. 91 (1953) 767.

/39/ V.N.Moskalev et al., Dokl. Akad.Nauk SSSR 110 (1956) 972.

/40/ D.V.Bugg et al., Rutherfor High Energy Laboratory Preprint RPP/h/13 (1966), Phys.Rev. 146 (1966) 980.

/41/ J.Bystricky et al., Lnadolt-Börnstein:Numerical Data and Functional Relationships in Science and Technology : ed. M.Schopper (Springer-Verlag, Berlin-Heidelberg-New York, 1980), New Series, Group I, 7 , p.15-21, 83.

/42/ R.Hofstadter et al., in Landolt-Börnstein: Numerical-Data and Functional Relationships in Science and Technology , ed. K.H.Hellwege (Springer-Verlag,Berlin, 1967), New Series, Group I, 2, p.21.

/43/ F.E.Rigia et al., Phys. Lett, 28 (1972) 185.

/44/ A.Ashmore et al., Proc. Phys. Soc. A71 (1958) 552.

/45/ H.P.Barett, Phys. Rev. 114 (1959) 1374.

/46/ M.S.Sinha et al., Phys.Rev. 105 (1957) 1587.

/47/ F.F.Chen et al., Phys.Rev. 99 (1955) 857.

/48/ T.Bowen, Nuovo Cim. 9 (1958) 908.

/49/ R.N.Vasilova et al., Izv. Akad, Nauk SSSR (Fiz.) 30 (1966) 1610.

/50/ A.Loret et al., Nuovo Cim. 31 (1964) 541.

/51/ Kh.Chernev et.al., XIII Intern. Conf. High Energy Physics, Berkeley University of California Press, (1966), paper 12a, 29.

/52/ M.H.MacGregor et al., Phys.Rev. 139B (1965) 362.

/53/ L.M.C.Dutton et.al., Phys.Rev.Lett 21 (1968) 1416.

/54/ N.Dalhajav et al., Yadern. Fiz. 8 (1974).

/55/ J.Bystricky et al., Landolt-Börnstein: Numerical Data and Functional Relationships in Science and Technology: ed. H.Schopper (Springer-Verlag Berlin-Heidelberg-New York, 1980) New Series, Group I, 9 , p.225, 289, 16.

TABLE CAPTIONS

Table 1a: The values of the parameters: γ_0 , γ_1 and χ^2/n_D, obtained by the fit of the total neutron - nucleus cross sections with eq.(4), the values of the total width $\Gamma = \Gamma_{np} A^{1/3}$ and the slope parameters b_{DDR} : eq. (7c), at $P_{LAB} = 4.2$ GeV/c.

Table 1b: The values of the parameters: γ_0 , γ_1 and χ^2/n_D obtained by the fit of the total neutron - nucleus cross sections with eq. (4); the values of the total width $\Gamma = \Gamma_{np} A^{1/3}$ and the slope parameter b_{DDR} : eq. (7c) at $P_{LAB} = 4.2$ GeV/c.

Table 2 : The values of the parameters: γ_0 γ_1 and χ^2/n_D obtained by the fit of the total proton-nucleus cross sections with eq. (4); the values of the total width $\Gamma = \Gamma_{np} A^{1/3}$ and the slope parameter b_{DDR} : eq. (7c) at $P_{LAB} = 4.2$ GeV/c.

FIGURE CAPTIONS

Fig. 1 : The experimental data [41,51-55] on np scattering, for $p_{LAB} = 0.9 \div 10$ GeV/c are compared with the DDR predictions: eqs. (4) - (6) with the parameters obtained by the fit of the total cross sections (see the text).

Fig. 2 : The experimental data [18-25] on n ^{9}Be scattering for $p_{LAB} = 0.9 \div 10$ GeV/c , are compared with the DDR predictions: eqs. (4) - (6) with the parameters obtained, by the fit of the total cross sections (see the text).

Fig. 3 : The experimental data [18-29,44] on n ^{12}C scattering, for $p_{LAB} = 0.9 \div 10$ GeV/c , are compared with the DDR predictions: eqs. (4) - (6) with the parameters obtained by the fit of the total cross sections and with $R = 3.19$ fm (full lines) and $R = 2.95$ fm (dashed lines).

Fig. 4 : The experimental data [18-29,44,45] on n ^{27}Al scattering, for $p_{LAB} = 0.9 \div 10$ GeV/c , are compared with the DDR predictions: eqs. (4) - (6) with the parameters obtained by the fit of the total cross sections (see the text)

Fig. 5 : The experimental data [18,21-23] on n ^{56}Fe scattering, for $p_{LAB} = 0.9 \div 10$ GeV/c , are compared with the DDR predictions: eqs. (4) - (6) with the parameters obtained by the fit of the total cross sections (see the text).

Fig. 6 : The experimental data [18-29], [44,46] on $n\,Cu$ scattering, for $P_{LAB} = 0.9 \div 10\ GeV/c$, are compared with the DDR predictions: eqs. (4) - (6) with the parameters obtained by the fit of the total cross sections and with $R = 5.01\ fm$ (full lines) and $R = 4.80\ fm$ (dashed lines).

Fig. 7 : The experimental data [19,22], [26,28,44] on $n\,Sn$ scattering, for $P_{LAB} = 0.9 \div 10\ GeV/c$, are compared with the DDR predictions: eqs. (4) - (6) with parameters obtained by the fit of the total cross sections (see the text).

Fig. 8 : The experimental data [18-26], [28,29,44,45] on $n\,^{207}Pb$ scattering, for $P_{LAB} = 0.9 \div 10\ GeV/c$ are compared with the DDR predictions: eqs. (4) - (6) with parameters obtained by the fit of the total cross sections and with $R = 7.15\ fm$ (full lines), $R = 7.30\ fm$ (dashed lines).

Fig. 9 : The experimental data [40,55] on pD scattering, for $P_{LAB} = 0.9 \div 10\ GeV/c$ are compared with the DDR predictions: eqs. (4) - (6) with parameters obtained by the fit of the total cross sections and with $R = 2.0\ fm$ (full lines) and $R = 2.2\ fm$ (dashed line).

Fig.10 : The experimental data [30-33,23-25] on $p\,^{4}He$ scattering, for $P_{LAB} = 0.9 \div 10\ GeV/c$ are compared with the DDR predictions: eqs. (4) - (6) with parameters obtained by the fit of the total cross sections (see the text).

Fig.11 : The experimental data [30] , [33-39,45,47-50] on pC scattering, for $P_{LAB} = 0.9 \div 10$ GeV/c, are compared with the DDR predictions: eqs. (4) - (6) with the parameters obtained by the fit of the total cross sections and with R=3.19 fm (full lines) and R=2.95 fm (dashed lines).

Fig.12 : The experimental data [40] on $p\,^{27}Al$ scattering, for $P_{LAB} = 0.9 \div 10$ GeV/c , are compared with the DDR predictions: eqs. (4) - (6) with parameters obtained by the fit of the total cross sections and with R=3.76 fm (full lines) and R= 3.90 fm (dashed lines).

Fig.13 : The experimental data [43] on the logarithmic slopes of the neutron-nucleus forward peak at $P_{LAB} = 4.2$ GeV/c are compared with the DDR predictions: eq. (7c) with R fixed as in table 2.

Fig.14 : The parameters γ_0 and γ_1 , obtained by the fit of the total cross sections, are compared with the curves described by: $\gamma_0 = (2.322 \pm 0.014)\, A^{0.483 \pm 0.002}$ (full line) and $\gamma_1 = (0.650 \pm 0.004)\, A^{0.572 \pm 0.002}$ (dashed line).

TABLE 1a

nA	R_A (fm)	γ_0	γ_1	Γ (GeV)	$b(GeV^{-2})$	χ^2/n_D	Refs.
np	0.930	1.961±0.028	1.699±0.002	5.6784±0.2123	7.79	4.31	[41]
	1.034 [42]	2.203±0.028	1.443±0.002		9.36	3.94	
	1.15	2.434±0.029	1.220±0.001		11.30	3.78	
$^{9}_{n}Be$	3.12 [42]	7.039±0.105	2.223±0.013	11.812	66.9	1.18	[18-25]
	3.9	7.065±0.106	2.120±0.012		70.3	1.17	
$^{12}_{n}C$	2.95	7.833±0.070	3.277±0.010	13.000	59.5	1.44	[18-27]
	3.19 [42]	7.923±0.069	2.830±0.009		69.4	1.42	
	3.27	7.951±0.069	2.701±0.008		72.8	1.41	
$^{27}_{n}Al$	3.66	11.607±0.081	5.446±0.024	17.035	89.6	1.68	[18-28]
	3.76 [42]	11.640±0.081	5.174±0.023		94.5	1.68	
	3.84	11.767±0.081	4.971±0.022		98.5	1.68	
$^{56}_{n}Fe$	4.84	16.089±0.178	7.078±0.045	21.725	154.4	2.26	[18,21-23]
	4.97 [42]	16.125±0.207	6.719±0.043		162.9	2.26	

TABLE 1b

nA	R_A (fm)	γ_0	γ_1	Γ (GeV)	b (GeV^{-2})	χ^2/n_D	Refs
nNi	4.92	18.350±1.097	7.481±0.128	22.106	159.5	0.15	[21,22]
nCu	4.80	17.480±0.174	8.481±0.043	22.714	152.0	2.05	[18-28]
	5.01	17.541±0.040	7.810±0.040		165.4	2.06	
nZn	5.1	20.977±1.691	8.293±0.249	22.831	171.1	0.17	[21,22]
nAg	5.93	26.478±1.753	10.225±0.211	26.958	230.2	0.31	[21,22,24]
nSn	5.99 [42]	25.610±1.479	10.907±0.172	27.930	234.8	0.49	[19-22,26,28,29]
nPb	6.98 [42]	26.811±0.476	14.077±0.150	33.590	318.0	0.80	[18-26]
	7.15	26.843±0.434	13.432±0.143		333.5	0.80	
	7.30	26.872±0.4	12.899±0.138		345.7	0.80	
nBi	6.87 [42]	32.847±1.907	15.528±0.342	33.698	307.9	0.83	[20-22]
	7.15 [42]	32.917±1.910	14.365±0.317		333.3	0.83	
^{238}nU	7.75	30.699±0.652	13.772±0.084	35.190	391.2	1.65	[18.19]
	8.15	38.52 ±0.675	15.471±0.076		432.4	1.65	[21-23,25]
nD	1.4	2.815±0.019	1.968±0.001	7.1543	15.42	172.65	[41]
	1.8	3.222±0.020	1.275±0.001		24.59	153.8	
	2.2	3.497±0.020	0.892±0.001		35.89	142.5	

TABLE 2

nA	R_A (fm)	γ_0	γ_1	Γ (GeV)	$b(GeV^{-2})$	χ^2/n_D	Refs.
pD	2.0	6.854±0.622	1.576±0.160	10.016±0.846	29.1	6.41	[40]
	2.2	2.624±0.071	0.609±0.011	4.726±0.087	37.6	11.2	
pHe	2.21 [42]	4.326±0.145	1.665±0.007	9.014	35.3	2.89	[30-33] [23,25]
pC	2.95	7.698±0.305	3.320±0.015	13.000	59.6	1.95	[30,33-39]
	3.19 [42]	7.801±0.310	2.867±0.015		69.4	1.94	
pO	3.55 [42]	8.217±0.495	3.241±0.013	14.309	85.3	2.75	[30]
pAl	3.76 [42]	12.202±0.082	5.503±0.019	17.035	94.5	0.84	[40]
	3.84	12.223±0.082	5.286±0.018		98.5	0.83	
	3.90	12.245±0.082	5.132±0.018		101.5	0.83	

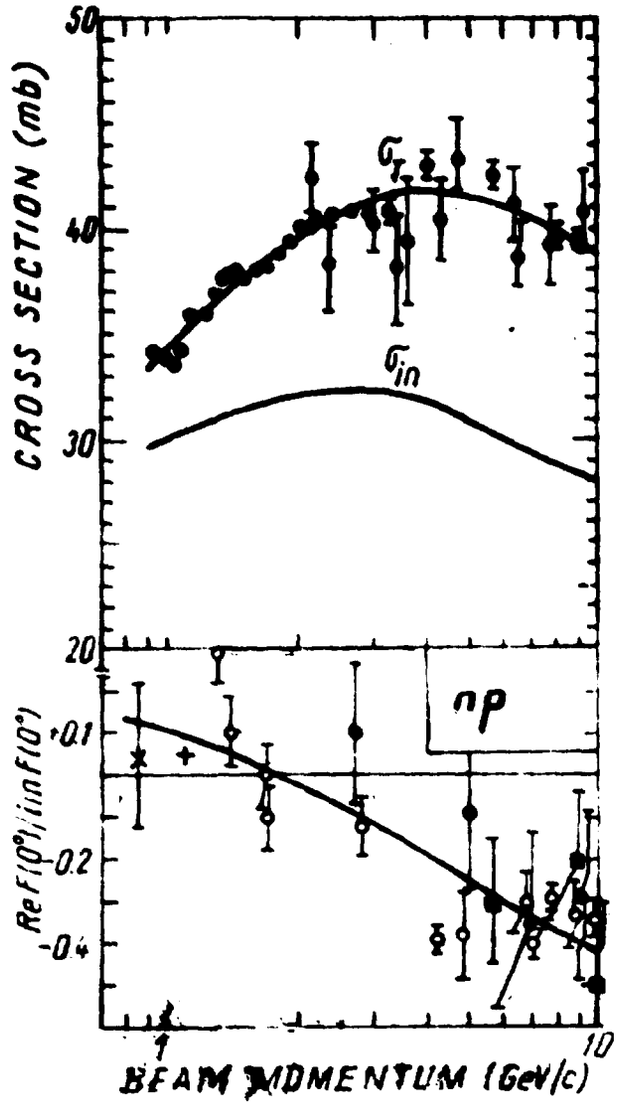
CROSS SECTION (mb)
50
40
30
20
σ_T
σ_{in}
np
0.1
0.2
0.4
1
10
BEAM MOMENTUM (GeV/c)

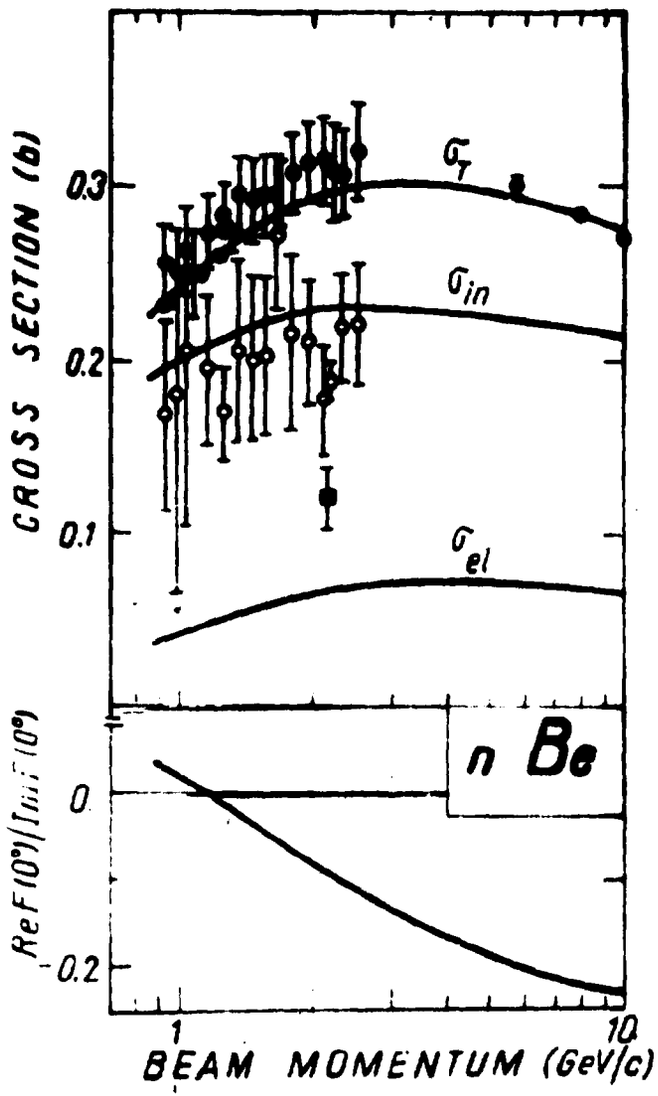
CROSS SECTION (b)
0.3
0.2
0.1
σ_T
σ_{in}
σ_{el}
n Be
0
0.2
1
10
BEAM MOMENTUM (GeV/c)

Fig. 2

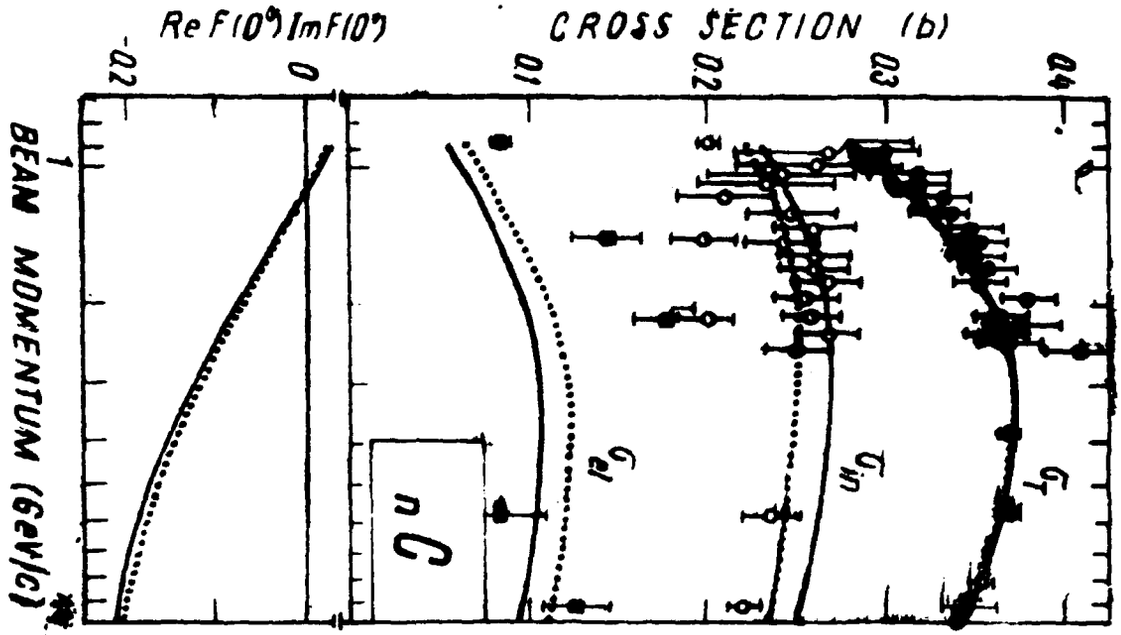
Re F(0°) Im F(0°)
CROSS SECTION (b)
-0.2
0
0.1
0.2
0.3
0.4
1
BEAM MOMENTUM (GeV/c)
n C
σ_{el}
σ_{in}
σ_T

Fig. 3

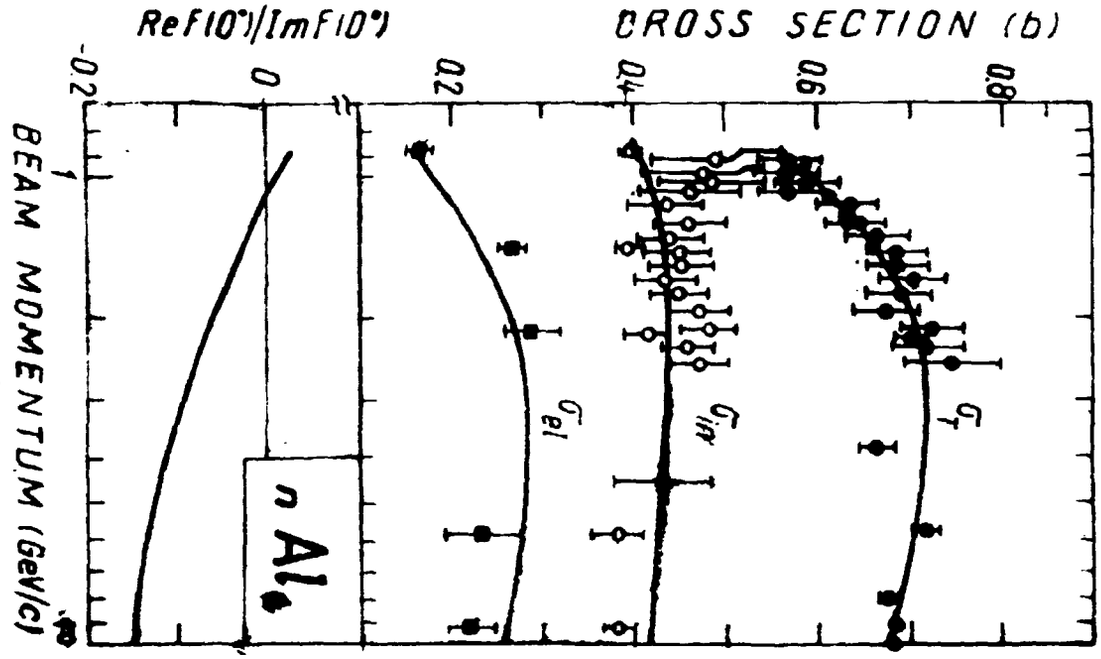
Re F(0°)/Im F(0°)
CROSS SECTION (b)
-0.2
0
0.2
0.4
0.6
0.8
1
BEAM MOMENTUM (GeV/c)
n Al
σ_{el}
σ_{in}
σ_T

Fig. 4

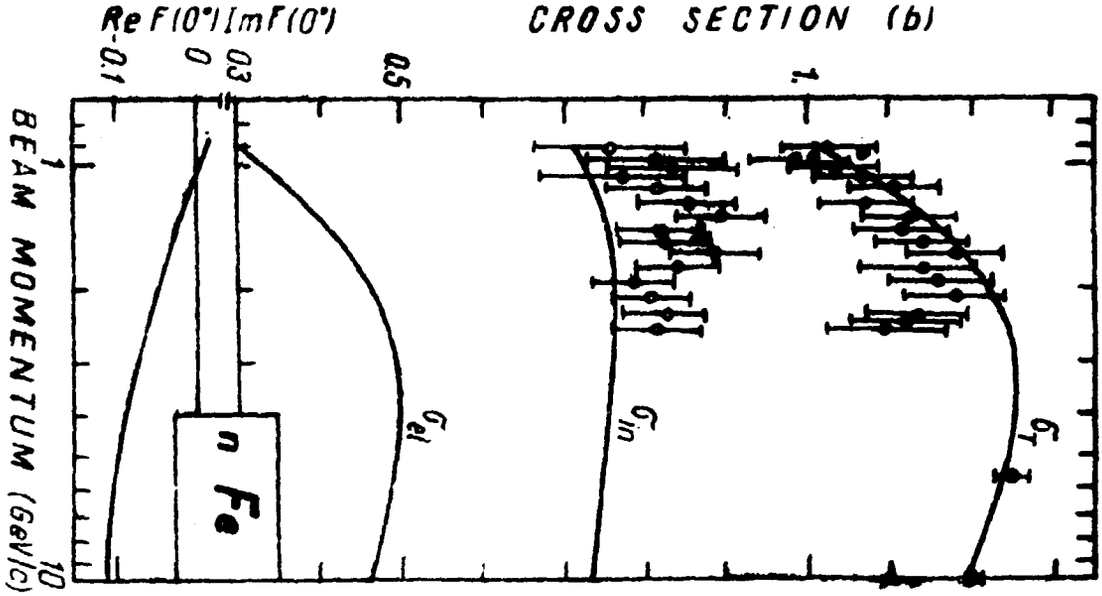
Re F(0°)/Im F(0°)
CROSS SECTION (b)
-0.1
0
0.3
0.5
1.
BEAM MOMENTUM (GeV/c)
1
10
n Fe
σ_{el}
σ_{in}
σ_T

Fig. 5

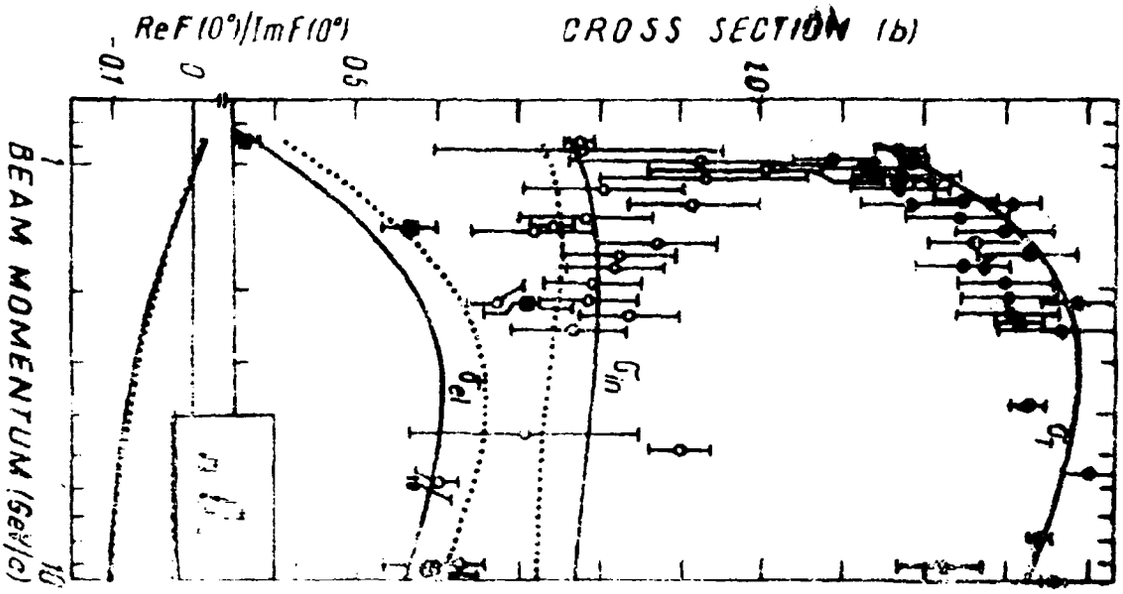
Re F(0°)/Im F(0°)
CROSS SECTION (b)
-0.1
0
0.5
1.0
BEAM MOMENTUM (GeV/c)
1
10
σ_{el}
σ_{in}
σ_T

Fig. 6

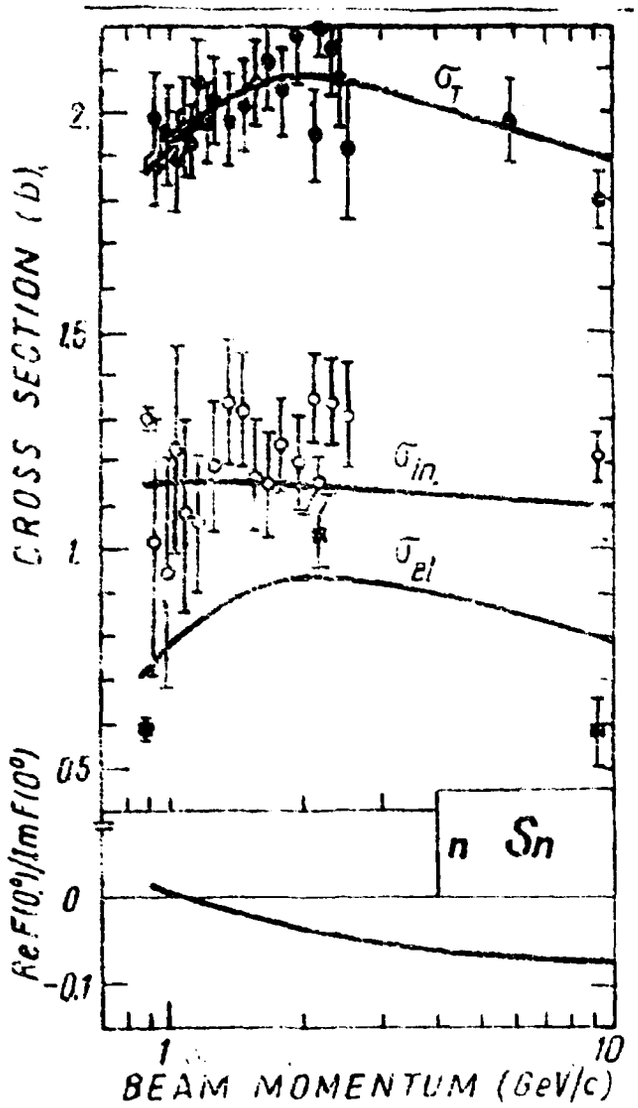
CROSS SECTION (b)
σ_T
σ_{in}
σ_{el}
n Sn
Re F(0°)/Im F(0°)
BEAM MOMENTUM (GeV/c)

Fig. 7

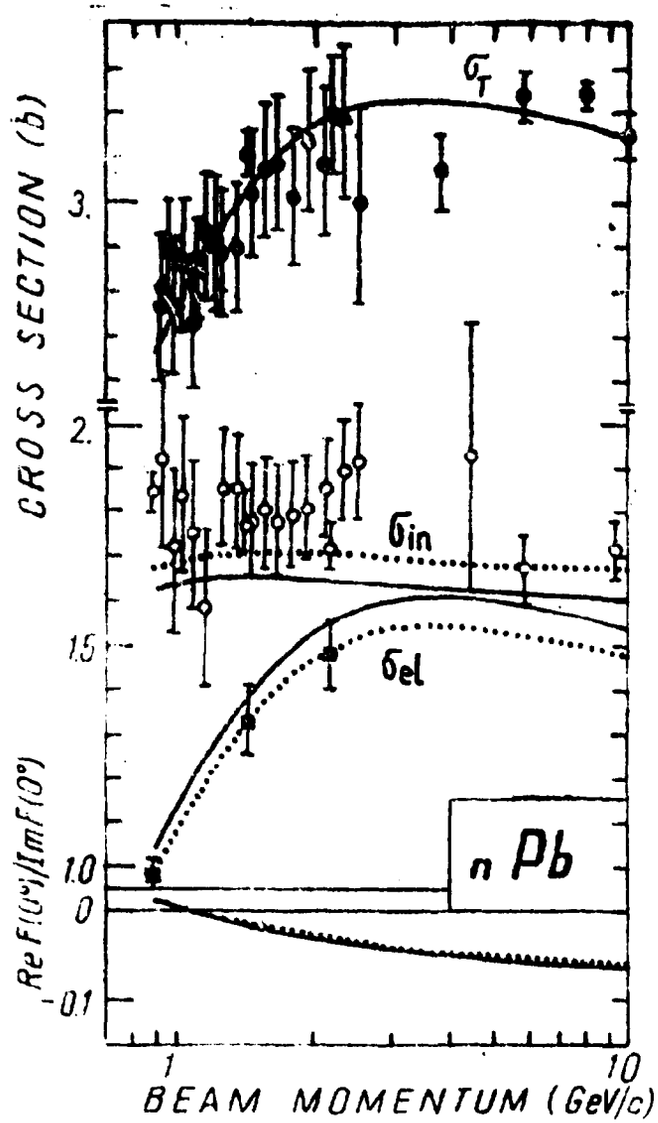
CROSS SECTION (b)
σ_T
σ_{in}
σ_{el}
n Pb
Re F(0°)/Im F(0°)
BEAM MOMENTUM (GeV/c)

Fig. 8

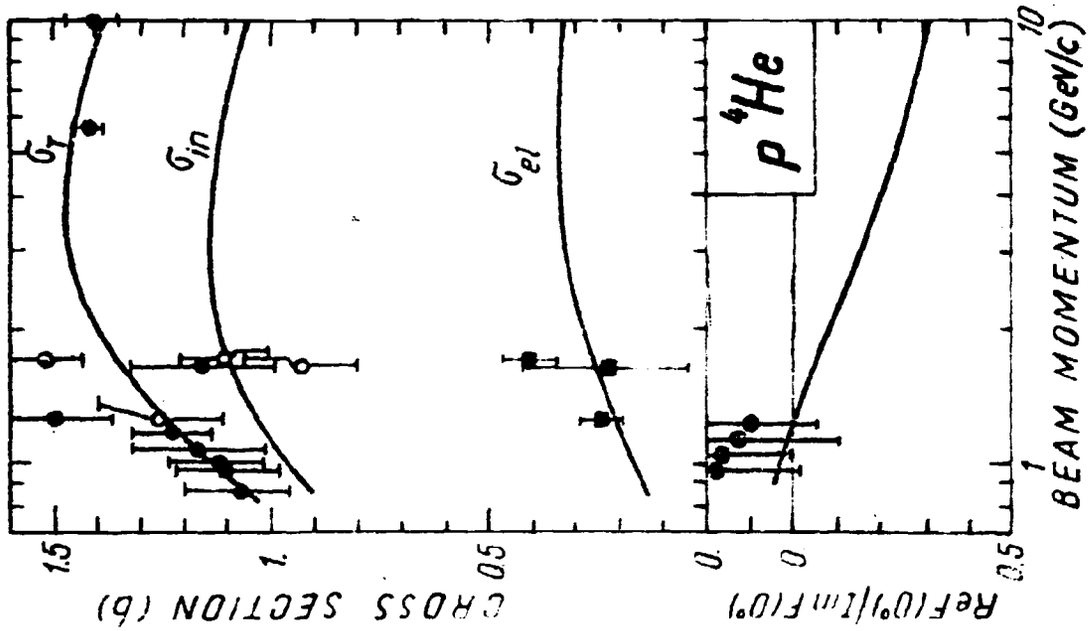
p ⁴He
σT
σin
σel
CROSS SECTION (b)
Re f(0°)/Im f(0°)
BEAM MOMENTUM (GeV/c)

Fig. 10

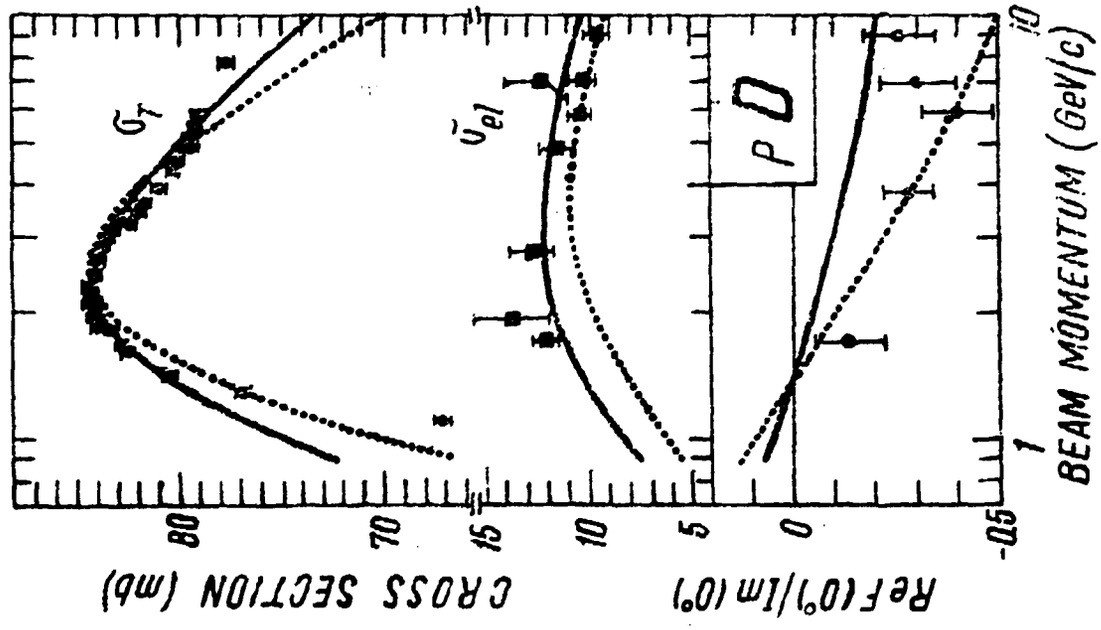
p D
σT
σel
CROSS SECTION (mb)
Re f(0°)/Im f(0°)
BEAM MOMENTUM (GeV/c)

Fig. 9

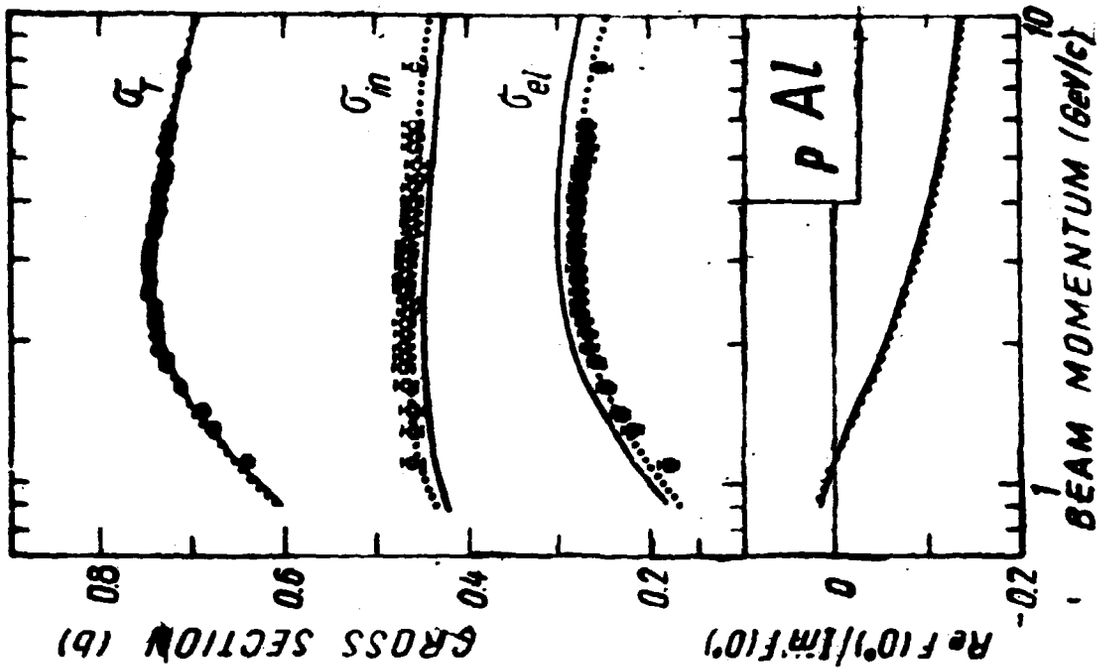
p Al
σ_T
σ_{in}
σ_{el}
GROSS SECTION (b)
Re f(0°)/Im f(0°)
BEAM MOMENTUM (GeV/c)

Fig. 12

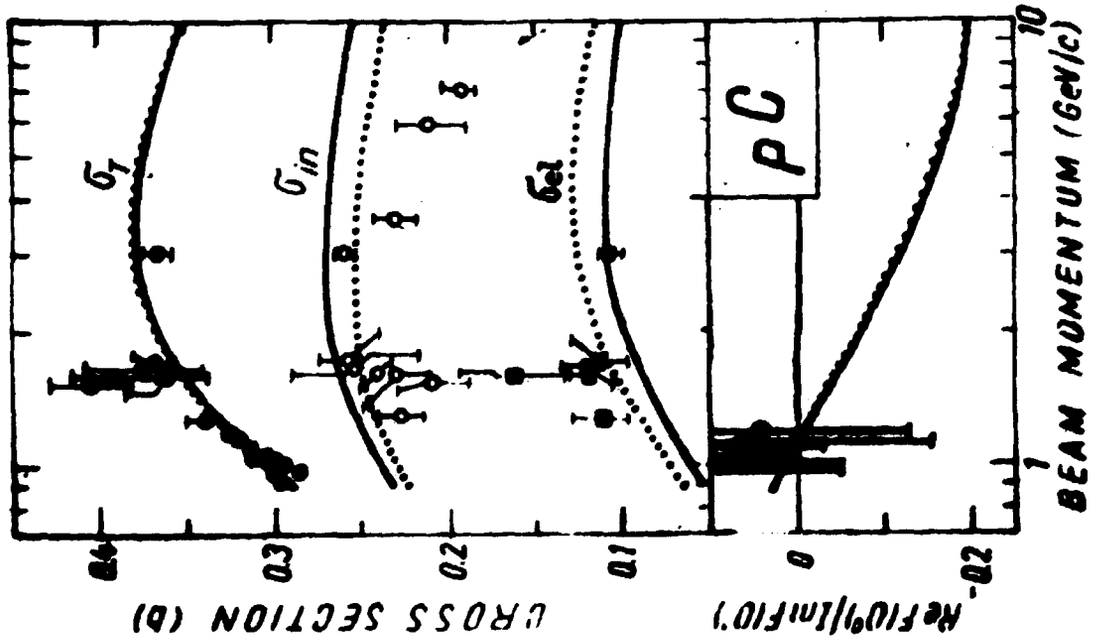
p C
σ_T
σ_{in}
σ_{el}
GROSS SECTION (b)
Re f(0°)/Im f(0°)
BEAM MOMENTUM (GeV/c)

Fig. 11

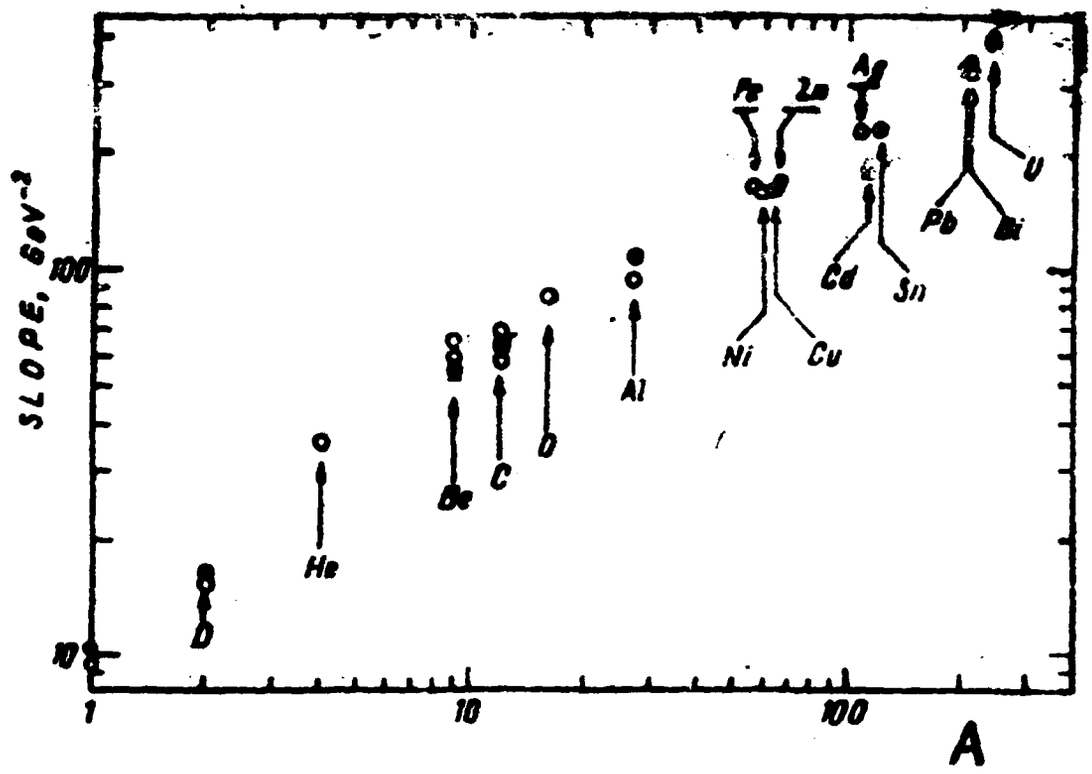
SLOPE, GeV⁻²
100
10
1
10
100
A
D
He
Be
C
O
Al
Ni
Cu
Zn
Cd
Sn
Pb
Bi
U

Fig. 13

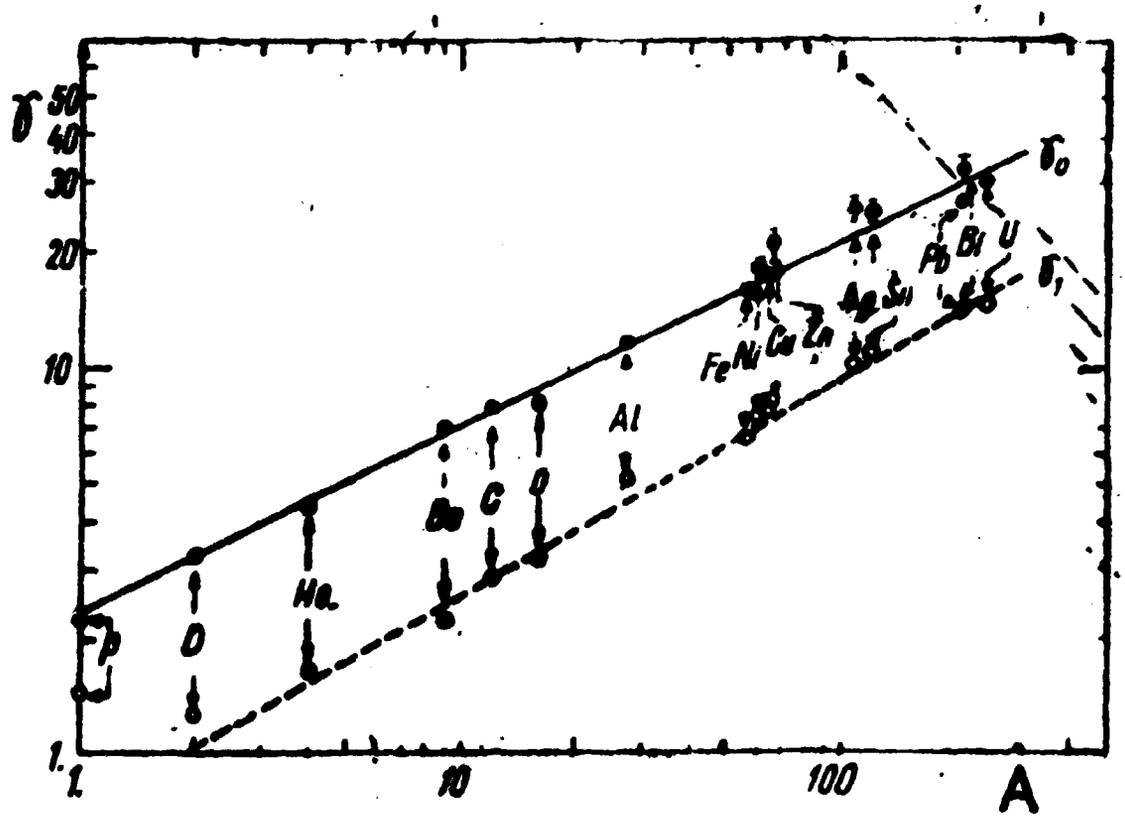
γ
50
40
30
20
10
1.
1.
10
100
A
γ₀
γ₁
p
D
He
Be
C
O
Al
Fe
Ni
Cu
Zn
Pb
Bi
U

Fig. 14